TU Delft

Delft University of Technology

Electrochemical Oxidation of Organic Pollutants Powered by a Silicon-Based Solar Cell

Perez-Rodriguez, Paula; Maqueira Gonzalez, Carlos; Bennani, Yasmina; Rietveld, Luuk C.; Zeman, Miro; Smets, Arno H.M.

DOI
10.1021/acsomega.8b02502

Publication date
2018

Document Version
Final published version

Published in
ACS Omega

Citation (APA)
Perez-Rodriguez, P., Maqueira Gonzalez, C., Bennani, Y., Rietveld, L. C., Zeman, M., & Smets, A. H. M. (2018). Electrochemical Oxidation of Organic Pollutants Powered by a Silicon-Based Solar Cell. *ACS Omega*, *3*(10), 14392-14398. https://doi.org/10.1021/acsomega.8b02502

Important note
To cite this publication, please use the final published version (if applicable).
Please check the document version above.

Copyright
Other than for strictly personal use, it is not permitted to download, forward or distribute the text or part of it, without the consent of the author(s) and/or copyright holder(s), unless the work is under an open content license such as Creative Commons.

Takedown policy
Please contact us and provide details if you believe this document breaches copyrights.
We will remove access to the work immediately and investigate your claim.

This work is downloaded from Delft University of Technology.
For technical reasons the number of authors shown on this cover page is limited to a maximum of 10.

This is an open access article published under a Creative Commons Non-Commercial No Derivative Works (CC-BY-NC-ND) Attribution License, which permits copying and redistribution of the article, and creation of adaptations, all for non-commercial purposes.

ACS OMEGA

Article

Cite This: ACS Omega 2018, 3, 14392−14398

http://pubs.acs.org/journal/acsodf

Electrochemical Oxidation of Organic Pollutants Powered by a Silicon-Based Solar Cell

Paula Perez-Rodriguez,*[,†] Carlos Maqueira Gonzalez,[†] Yasmina Bennani,[‡] Luuk C. Rietveld,[‡] Miro Zeman,[†] and Arno H. M. Smets[†]

[†]Photovoltaic Materials and Devices (PVMD), Electrical Engineering, Mathematics and Computer Science Faculty and [‡]Sanitary Engineering, Civil Engineering Faculty, Delft University of Technology, 2628 CD Delft, The Netherlands

ABSTRACT: Currently available (photo-)electrochemical technologies for water treatment establish a trade-off between low-pollutant concentration and costs. This paper aims at decoupling these two variables by designing a photo-oxidation device using earth abundant materials and an electronic-free approach. The proposed device combines a graphite/graphite electrochemical system with a silicon-based solar cell that provides the necessary electrical power. First, the optimum operational voltage for the graphite/graphite electrochemical system was found to be around 1.6 V. That corresponded closely to the voltage produced by an a-Si:H/a-Si:H tandem solar cell of approximately 1.35 V. This configuration was shown to provide the best pollutant degradation in relation to the device area, removing 70% of the initial concentration of phenol and 90% of the methylene blue after 4 h of treatment. The chemical oxygen demand (COD) removal of these two contaminants after 4 h of treatment was also promising, 55 and 30%, respectively. Moreover, connecting several solar cells in series led to higher pollutant degradation but lower COD removal, suggesting that the degradation of the intermediate components is a limiting factor. This is expected to be due to the higher currents achieved by the series-connected configuration, which would favor other reactions such as polymerization over the degradation of intermediate species.

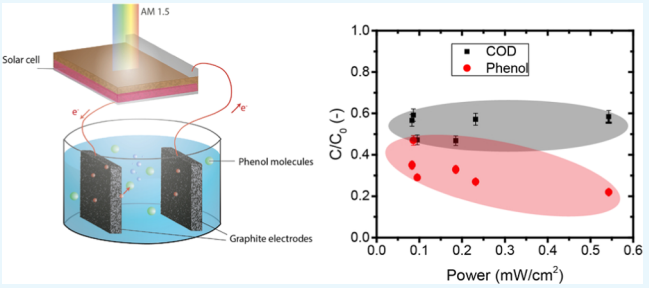

1. INTRODUCTION

Clean water scarcity is expected to be one of the main challenges for society in the near future,[1] with about a billion people with limited access to clean water.[2] The heavy industrialization and urbanization currently taking place are expected to increase the problem, polluting main water sources with hazardous effluents.[3] Some of the most common contaminants are organic pollutants, such as pesticides, pharmaceuticals, phenol compounds, chloroform, or dyes.[4,5] Several methods to remove organic contaminants include biological, physical, and chemical treatments.[6] However, these methods hardly remove the pollutants to the low concentrations needed.[7,8] Many advanced water treatment processes such as advanced oxidation processes (AOPs) are able to achieve low concentrations of contaminants but generally consume high amounts of energy.[8−10] Thus, the solution to tackle the polluted water problem should also take into account the device energy needs.

Electrochemical oxidation is a method with the potential to remove toxic organic compounds, ecologically hazardous cyanides, and other residual compounds even at low concentrations.[4,11] This method uses an electrical current provided by an external source to degrade the pollutants into less complex compounds such as CO_2, which are easier to remove by a post-treatment step.[12,13] Moreover, it can be coupled with devices based on earth-abundant materials that can cheaply provide the needed electrical energy to drive the process, eliminating the energy consumption impact of the whole device,[14] combining the advantages of low pollutant concentrations and low energy costs.

Previous work has demonstrated devices that can successfully degrade several organic contaminants using solar energy and earth-abundant materials using compounds such as bismuth-based compounds,[15,16] SnO_2,[1717] WO_3[18,19] and TiO_2.[20,2120,21] However, these materials are not able to effectively degrade organic pollutants using only solar energy. To tackle this challenge, previous research combined a $BiVO_4$ photoelectrode with a thin-film (TF) silicon solar cell and a graphite counter electrode.[22] The demonstrator device was able to effectively degrade phenol and cloroform, reducing the energy use from 4.21 W h/mg for the traditional TiO_2 to 0.79 W h/mg for the $BiVO_4$-based bias-free device. Nevertheless, this device is constrained by the interaction between the $BiVO_4$ and solar cell, since the solar spectrum needs to be distributed among the different junctions, and the produced current density would be limited by the photoanode. This paper aims at further decoupling these two subsystems by designing a solar cell based on earth-abundant materials that

Received: October 5, 2018
Accepted: October 18, 2018
Published: October 30, 2018

Downloaded via TU DELFT on November 22, 2018 at 13:02:01 (UTC).
See https://pubs.acs.org/sharingguidelines for options on how to legitimately share published articles.

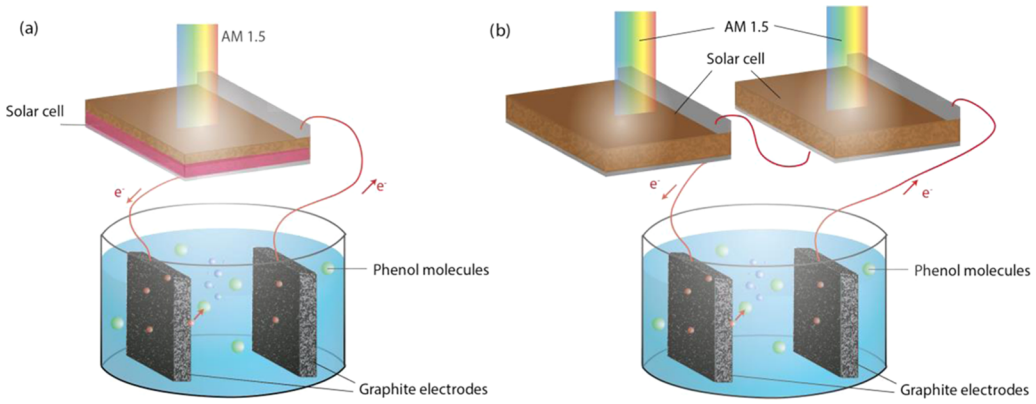

Figure 1. Schematic of a stand-alone device configuration combining an electrochemical system and (a) a solar cell, possibly multijunction, or (b) several solar cells connected in series, which can be either single or multijunction.

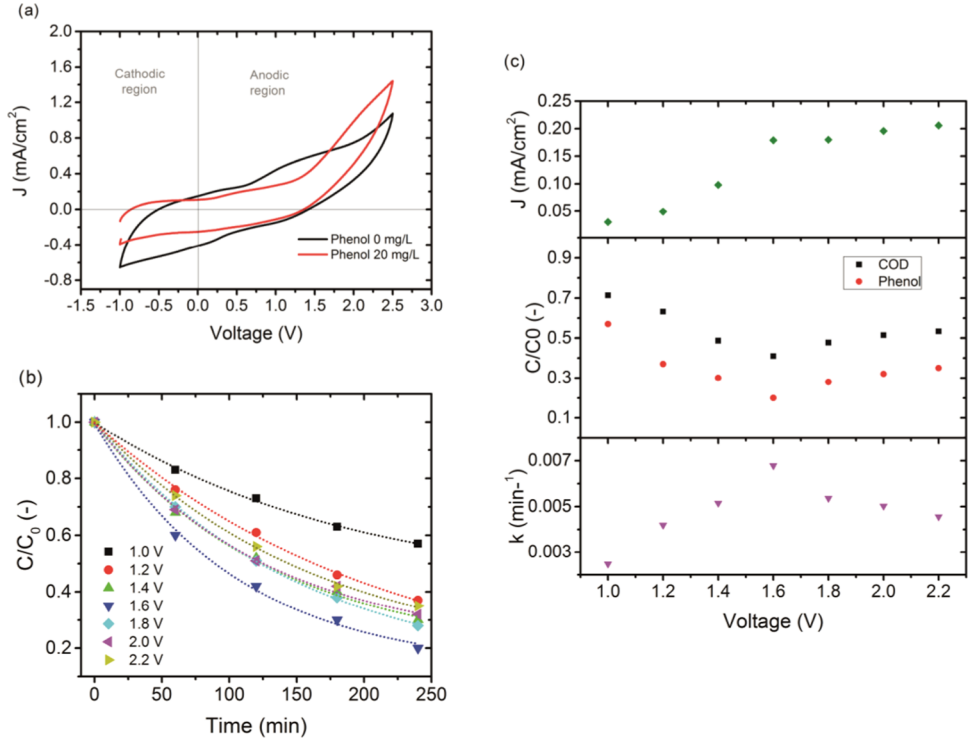

Figure 2. Characteristics of a graphite/graphite electrochemical system connected to a voltage source, (a) *JV* characteristics, (b) phenol degradation at different applied potentials, and (c) the corresponding first-order reaction constant; the current density measured flowing through the system at each voltage and the final concentration and COD in the sample after 4 h of degradation at different voltages.

can provide the necessary energy for a fully electrochemical system, without the inclusion of a photoelectrode. This configuration relaxes the requirements for the solar device, allowing for more flexibility of design. Moreover, by designing a direct solar water treatment system, no converter or inverter is needed, reducing the complexity of the system and the potential costs. However, there are some complex interactions at play. This study aims at analyzing the differences between using a solar cell and a voltage source to power the electrochemical system. The main parameters analyzed were the pollutant degradation and the chemical oxygen demand (COD).

Regarding the electrochemical system, different materials such as Ag, Al, Au, Cu, Ni, Pb, Pd, Pt, Ti, Zn, graphite, glassy carbon, and activated carbon fiber have been proposed in the literature as cathode materials in the electrochemical treatment of water containing different organic pollutants.[23] In this work, two graphite plates were studied due to their relative low cost with respect to other more precious metals and relatively high removal efficiency.[4]

The materials available regarding the photovoltaic (PV) cell implementation include III−V technologies, perovskites, organics, crystalline silicon (c-Si), TF amorphous and nanocrystalline silicon (a-Si:H and nc-Si:H), and copper indium gallium selenide (CIGS).[24,25] The technological choice depends on the design requirements of the electrochemical components. The voltage characteristics of the used electrodes must be taken into account as one of the main variables affecting the solar cell choice. However, unlike other configurations such as that of an external power source, solar cells are also current sources and thus the current−voltage interaction would play an important role on the final

DOI: 10.1021/acsomega.8b02502
ACS Omega 2018, 3, 14392−14398

performance. Thin-film silicon and crystalline silicon technologies have been chosen as the preferred PV technologies due to their relatively low cost, availability, and design flexibility. Here, several different PV technologies and configurations have been studied, including a-Si:H, nc-Si:H, and silicon heterojunction (SHJ) solar cells. In addition, either monolithic multijunction solar cells (Figure 1a) or wired series-connected solar cells (Figure 1b) may be required to fulfill the voltage requirements of the oxidation process.[26−28]

By decoupling the two elements of charge carrier generation and collection and the redox reactions, each element can be better optimized. Thus, the resulting device would have the potential to reduce the costs of advanced water treatment processes by using free solar energy and earth-abundant materials and have the additional advantage of being electrically autonomous from any external power source. However, to achieve such efficient devices, the interaction between the current and voltage produced by the solar cell and the electrochemical system must be better understood and compared with the more common case of an independent power source.

2. RESULTS AND DISCUSSION

A device consisting of a solar cell and an electrochemical system for the degradation of organic pollutants in water was studied. To understand and improve the performance of the proposed system, the electrochemistry of the graphite plate system was analyzed first. Then, different solar cell configurations were designed on the basis of the identified electrochemical characteristics. The solar cells were separately characterized and then combined with the electrochemical system. The potential of this stand-alone device to effectively remove organic contaminants was then determined.

2.1. Electrochemical System Characterization. The electrochemical system, in this context, refers to the part of the system comprised by the two electrodes and the electrolyte. The interaction between the electrochemical oxidation and reduction reactions is crucial to characterize the system, and it can help to minimize the overpotential related to the electrodes. In this work, two graphite plates were studied due to their relative low cost with respect to other more precious metals and high removal efficiency.[4] Figure 2a shows the *JV* characteristics of the graphite/graphite electrochemical system. The system shows a rather high hysteresis loop between −1 and 2.5 V. This effect could be related to the capacitance created between the two electrodes due to the charge-transfer barriers between the electrodes and the electrolyte. In addition, no characteristic peak could be observed for the formation of any intermediate compound. Previous research also has related the absence of this peak in graphite electrodes to the fouling effect of phenol, which passivates the electrode.[29,30] Thus, to determine if the phenol reaction occurs, Figure 2a also compares the *JV* characteristics of the system with and without phenol present in the solution. When phenol was introduced, the current at positive voltages increased, which confirms the phenol degradation at voltage ranges between 1 and 2.5 V. Moreover, a lower hysteresis can be observed when phenol was present, indicating that the charges can be more easily transferred to the electrolyte. To further optimize the voltage response of the system, degradation experiments were conducted using different potentiostat-applied voltages ranging from 1 to 2.2 V. The results are shown in Figure 2b. The concentration profiles observed correspond to a first-order reaction, allowing to calculate the reaction rate constant, as plotted in Figure 2c. The R^2 value of the fitting in this case was always higher than 0.99. The reaction rate constant shows a clear maximum at 1.6 V, which also coincides with the minimum concentration and COD in the solution after 4 h of treatment. When operating below this voltage of 1.6 V, the charge carrier density was not enough to produce many radicals and degrade the phenol molecules. This is indicated by the trends in the current density, which steadily increased with voltage up to 1.6 V. After this voltage, the current density stabilized, indicating that the charge carrier generation and separation inside the graphite were not the limiting factors anymore. The degradation efficiency decreased after this point due to other competing reactions such as water splitting. Compared to other similar systems such as TiO_2-based systems, the voltage needed is higher for achieving similar currents due to the photoactivity of TiO_2.[31] However, in the proposed system, that photoactivity is transferred to the solar cell, avoiding issues associated to light absorption in the solution.

The solar cell designed to be integrated in this device should have an operational voltage around 1.6 V to assure charge carrier separation inside the semiconductor and at the same time to not surpass the water splitting reaction potential, which would reduce the availability of charges for the phenol degradation reaction. Instead, it is expected that OH radicals are produced at this voltage.[22] To confirm the suitability of this electrochemical system for other contaminants, the degradation of methylene blue was also tested. Quantitatively, the absorbance of the solution was measured to evaluate the methylene blue removal, as shown in Figure 3. In particular,

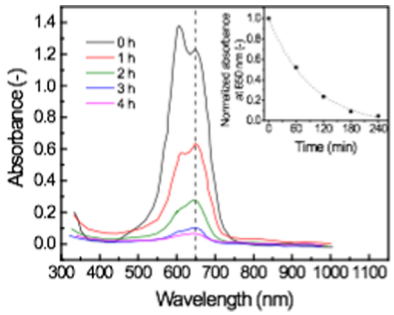

Figure 3. Degradation of methylene blue with an applied voltage of 1.6 V, measured by the absorbance peak change with time.

the peak at a wavelength of 650 nm was used to evaluate the dye removal due to its more persistent nature.[32] A reduction of the methylene blue concentration similar to previous works was achieved,[33] achieving almost complete removal after 4 h of degradation, as observed, confirming the suitability of these systems for a variety of organic contaminants. Moreover, this system would be able to outperform the traditional TiO_2 photoelectrodes,[34] since the light absorption in the methylene blue does not affect the graphite/graphite performance, unlike for TiO_2.

2.2. Solar Cell Characterization. To achieve the desired potential of 1.6 V, a solar device was coupled to the electrochemical system. TF silicon solar cells and silicon heterojunction (SHJ) cells were used due to their flexibility of design, their low costs, and their high performance. When using TF silicon, a multijunction approach can be used, allowing for higher operational voltages than single junctions

DOI: 10.1021/acsomega.8b02502
ACS Omega 2018, 3, 14392−14398

and better spectral utilization. The absorber thicknesses were adjusted to optimize the output parameters, setting as boundary condition that the a-Si:H top absorber layers would not increase further than 300 nm to avoid strong light-induced degradation.[35] In addition, flat silicon heterojunction (SHJ) solar cells are also available. The main external parameters obtained for each of the available cells are summarized in Table 1.

Table 1. External Parameters of the Selected Thin-Film Solar Cells at Standard Test Conditions (STC)

solar cell type	V_{OC} (V)	J_{SC} (mA/cm^2)	efficiency (%)	FF
a-Si:H	0.85	18.7	9.9	0.62
a-Si:H/nc-Si:H	1.36	12.9	10.5	0.60
a-Si:H/a-Si:H	1.67	8.88	9.04	0.61
SHJ	0.68	35.00	12.85	0.54

Some of these cells produced a voltage close to the optimum operational voltage previously determined, namely, a-Si:H/nc-Si:H and a-Si:H/a-Si:H cells. Thus, these cells could be tested as a single multijunction device. However, since most of the used solar cells have operational voltages lower than the optimum 1.6 V, several cells must be connected in series. Here, two a-Si:H, two SHJ, two a-Si:H/nc-Si:H, and two a-Si:H/a-Si:H were connected in series to achieve higher voltages. Note that, even though the performance of these cells might be superior, the solar cell area is doubled related to that of the individual cells. Thus, a direct cost-performance comparison between the two configurations is not possible.

2.3. Electrochemical System Powered by a Solar Cell. To determine the suitability of these strategies for water treatment, the solar cells were coupled to the electrochemical system previously described, resulting in the phenol and methylene blue degradation characteristics shown in Figure 4. Looking at the individual cells, it can be seen that with an a-Si:H/a-Si:H double junction solar cell, a better degradation was reached in comparison to the case of a-Si:H/nc-Si:H. The a-Si:H/a-Si:H cells were able to produce a higher operational voltage, injecting charge carriers more efficiently into the solution to drive the phenol degradation reaction.[36] The produced current density remained within the same order of magnitude for the two cells. When adding several of these cells in series, higher operational voltages were achieved, closer to the desired value of 1.6 V. This resulted in a higher phenol degradation for the case of two a-Si:H/nc-Si:H in series, reducing the phenol concentration by 80% after 4 h. In the case of methylene blue, all cells in series achieved values similar to the ones for the individual a-Si:H/a-Si:H cells, reaching low dye concentrations. Overall, connecting several cells in series did not significantly improve the performance, since in most cases, the voltage obtained was too high for optimum operation, and the possible mismatches between cells can further lower the performance.

Moreover, even though the system with the two a-Si:H/nc-Si:H cells connected in series showed the best pollutant degradation, it resulted in the highest remaining COD values after 4 h of degradation. The lowest final COD values for phenol correspond to the individual a-Si:H/a-Si:H cell and the two SHJ cells in series. For methylene blue, the lowest values were achieved with the individual a-Si:H/a-Si:H cell and the two a-Si:H cells in series. Thus, it seems that after a certain voltage threshold, higher operational voltages can lead to lower COD removal. Overall, considering the achieved pollutant degradation and COD removal, as well as the needed PV area, an a-Si:H/a-Si:H tandem solar cell appeared to be the most viable option, achieving a phenol removal of 70% (energy use of 0.19 W h/mg phenol), a methylene blue removal of 90% (energy use of 0.12 W h/mg methylene blue), and COD removals of these two pollutants of 55 and 30%, respectively. Moreover, compared to the energy use of 0.79 W h/mg phenol for a $BiVO_4$ photoanode connected to a solar cell,[22] decoupling

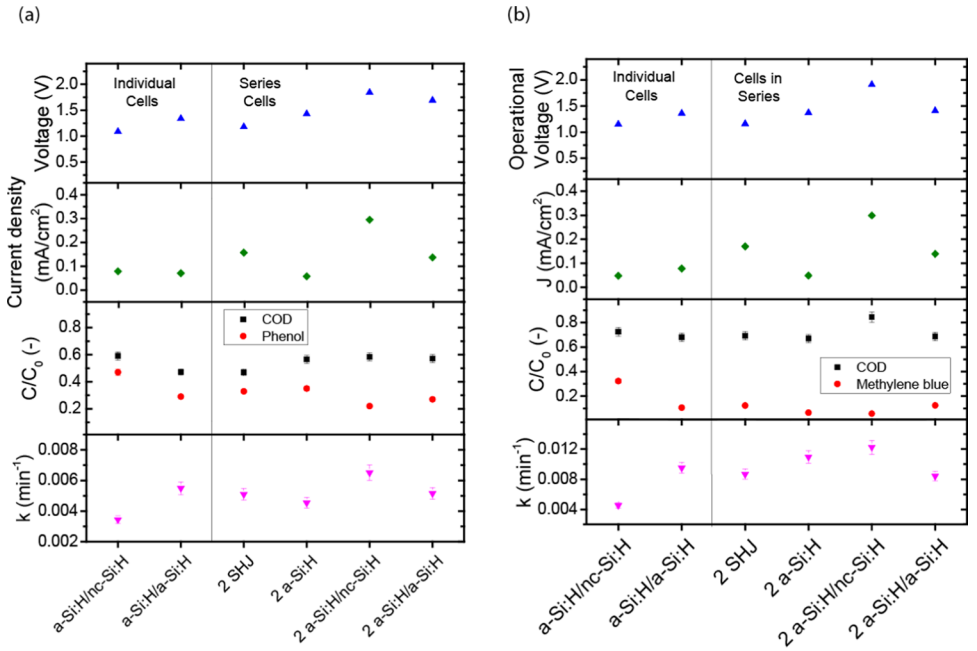

Figure 4. (a) Phenol and (b) methylene blue degradation characteristics when using different solar cells. The current densities reported are based on the electrode area of 16 cm^2.

DOI: 10.1021/acsomega.8b02502
ACS Omega 2018, 3, 14392−14398

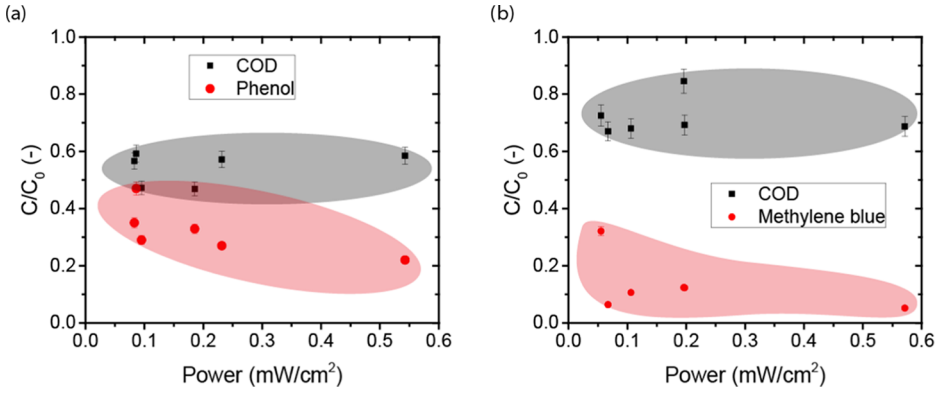

Figure 5. Concentration of (a) phenol and (b) methylene blue and their respective CODs after 4 h of degradation with respect to the power provided by the different solar cell configurations. The power densities refer to the areas of the electrodes, which are 16 cm^2 per electrode.

the PV and electrochemical elements seems to result in a more energy-efficient system.

When comparing the results of the solar cells (Figure 4) to those by voltage sources (Figure 2), some differences can be observed. In the case of solar cells, higher current densities can lead to lower COD, like for the two a-Si:H/nc-Si:H cells connected in series. This suggests that, since solar cells are not only voltage sources but also current sources, the current density must also be taken into account. To better understand this process, the COD concentrations and the final concentration of phenol and methylene blue are plotted as a function of the total power density provided by the solar cell, as depicted in Figure 5, calculated as the voltage times the current density of the solar cell under operation. This analysis shows that higher power densities resulted in a higher degradation of the organic molecules but a constant or slight increase in final COD, both for phenol and methylene blue. When the power density is high, the current densities are high at the surface of the electrode, and more contaminant molecules (phenol and methylene blue) are decomposed. However, the COD does not necessarily follow the same trend because it might need different voltages, current levels, or surface treatments, which would transfer these additional charge carriers to other side reactions, such as the creation of polymers that might cause fouling.[37] Therefore, the limiting factor is the degradation of the intermediate compounds, whose formation mechanisms have been studied elsewhere.[37,38] Although it could be argued that a factor leading to these results is the relatively low oxidation potential of the graphite electrodes, this effect was not seen when using the same electrodes connected to a voltage source and therefore other effects must be present.

3. CONCLUSIONS

A photo-oxidation device based on earth-abundant materials and solar illumination was successfully demonstrated. It consists of a graphite/graphite electrochemical system connected to a solar cell that provides the necessary electrical power. The optimum voltage for the graphite/graphite system was determined to be 1.6 V, at which it can efficiently degrade both phenol and methylene blue. A thin-film silicon solar cell was designed to operate at a voltage as close to this value as possible. An a-Si:H/a-Si:H tandem solar cell was found to give the best results, with phenol removal of 70% of the original concentration after 4 h of treatment. The limiting factor of these systems was determined to be the degradation of intermediate compounds by the solar cell system, since the COD after degradation was higher than that of the electrochemical device connected to a voltage source providing the same voltage. Connecting several of these cells in series did not significantly improve the performance, since the voltage obtained was too high for optimum operation and the mismatches between cells further lowered the performance. Moreover, normalizing of the results by the active PV area, using a single multijunction of a-Si:H/a-Si:H was the most suitable solution. In conclusion, an autonomous device consisting of an a-Si:H/a-Si:H solar cell combined to a graphite/graphite electrochemical system can provide an efficient way to remove organic pollutants from water, potentially reducing the costs and the greenhouse gas emissions of a water treatment facility.

4. MATERIAL AND METHODS

4.1. Solar Cell Fabrication. All TF solar cells were deposited by radio frequency plasma-enhanced chemical vapor deposition (RF-PECVD) using a cluster tool from Elettrorava. The a-Si:H and a-Si:H/a-Si:H solar cells were deposited on textured Asahi UV substrates, which use fluor-doped tin oxide (FTO) as transparent conductive oxide (TCO). The a-Si:H/nc-Si:H solar cells were deposited in wet-etched textured corning glass with aluminum-doped zinc oxide (AZO) as TCO. The texturing of the glass used for the a-Si:H/nc-Si:H cell is described elsewhere.[39] Nanocrystalline silicon oxide (nc-SiO_x:H) was used as p-layer (boron doped) and n-layer (phosphorous doped). The deposition rates of a-Si:H and nc-Si:H were 0.16 and 0.71 nm/s, respectively. The SHJ solar cells were deposited on a flat n⟨111⟩ float zone wafer from University Wafers cleaned by subsequent steps of HNO_3 and HF baths. Then, 7 nm of intrinsic a-Si:H were deposited in each side of the wafer, and 7 nm of p-type a-Si:H and 9 nm of n-type a-Si:H were fabricated to complete the structure. Finally, a 100 nm layer of low power and temperature indium-doped tin oxide was deposited on top of the p-type emitter layer as the front TCO. No TCO was used on the back of the solar cell.

The contacts for all cells have been deposited using electron beam physical vapor deposition. A 300 nm Al stripe in contact with the TCO has been used as a front contact. A stack of 200 nm Ag, 30 nm Cr, and 500 nm Al has been used as a back reflector and back contact. The solar cell area for all configurations was 1 cm^2. Interconnections have been performed by soldering Ag cables to the solar cell contacts.

DOI: 10.1021/acsomega.8b02502
ACS Omega 2018, 3, 14392−14398

4.2. Solar Cell Characterization. The external quantum efficiency (EQE) was measured in an inhouse setup in TU Delft, The Netherlands, to obtain the amount of charge carriers generated per photon at a given wavelength. The current density−voltage (*JV*) characteristics of the solar cells have been measured using a Wacom AAA solar simulator using two lamps (Xe and halogen) and an AM1.5 filter. The short-circuit current density has been corrected with the obtained value from the integration of the EQE weighted with the AM1.5 spectrum.

4.3. Photoelectrochemical Measurements and Sampling. Electrochemical experiments for phenol and dye degradation were carried out on a setup consisting of a cylindrical quartz glass reactor with an effective vessel volume of 200 mL, two graphite electrodes, and potentiostat (Autolab PGSTAT128N with a BOOSTER10A) connected to the electrochemical system to provide the needed voltage. The potentiostat was controlled by Nova Software, with a current accuracy of ±0.2%.[40] In experiments powered by solar energy, a solar cell was used, exposing it to an Atlas solar simulator (SUNTEST XXL+), aiming to achieve standard test conditions (STC) of 1000 W/m^2, AM1.5, and 25 °C.

The electrodes were graphite plates with an area of 16 cm^2 and were either connected to a solar cell or a voltage source. The initial volume of the working solution was 150 mL of either a phenol solution with initial concentration of 20 mg/L (≥99%, Sigma-Aldrich) or a 25 mg/L methylene blue solution (≥99%, Sigma-Aldrich). To eliminate the influence of solution resistance, 0.1 M Na_2SO_4 (≥99%, Merck) was chosen as supporting electrolyte. Demineralized water (RiOs 5 Reverse Osmosis System) was used throughout the experiments for dilution. At the start of each experiment, the graphite electrodes were kept in the stirred solution in the dark for 1 h for the adsorption at the electrode surface to reach equilibrium.[31] The pH of the solution was kept constant at 7.2 and was measured before the experiment, using a Sentix 81 pH meter. The temperature was controlled at 25 ± 1 °C by recirculating cooling water in a water bath equipped with cooler Julabo, FL300. During the experiments, the reactor was closed by a UV permeable quartz lid to prevent evaporation of phenol.

Samples of 2 mL of either phenol solution or dye solution were collected every hour for further characterization. Phenol reacts with 4-nitroaniline to form a yellow-colored complex, which is then measured using a UV−vis spectrophotometer (Hach Lange DR 3900, cuvette tests LCK 345 with a measuring range of 0.05−5.00, 5−50, and 20−200 mg/L). The possible measurement error of the spectrophotometer is ±5%.[41] The methylene blue absorption characteristics were also measured using the UV−vis spectrophotometer, and the characteristic peak at a wavelength of 650 nm was taken as an indication of the methylene blue concentration.[42]

The chemical oxygen demand (COD) describes the oxygen required to oxidize all soluble and particle organics. It gives an idea of the oxidation degree of the organic pollutants in the solution. The COD measurements were performed by using a mix containing a strong oxidizing agent ($Cr_2O_7^{2-}$), a small amount of silver for the more resilient organics, and mercury to avoid possible interaction with chloride ions. After adding the oxidizing agent, the samples were digested for 2 h and 148 °C, after which the amount of consumed oxidizing agent was determined. By subtracting the initial and final concentrations of the oxidizing agent present, the consumed oxidizing agent was determined. The accuracy of this method is considered by a standard error of ±5%.

AUTHOR INFORMATION

Corresponding Author

*E-mail: p.perezrodriguez@tudelft.nl.

Notes

The authors declare no competing financial interest.

ACKNOWLEDGMENTS

This work is part of the research programme of the Foundation for Fundamental Research on Matter (FOM-13CO19), which is part of the Netherlands Organisation for Scientific Research (NWO).

REFERENCES

(1) *Clean Energy Progress Report*; IEA, 2011.

(2) Worldbank. Access to electricity (% population), 2016. Available at https://data.worldbank.org/indicator/EG.ELC.ACCS.ZS.

(3) Qin, H.-P.; et al. Water Quality Changes during Rapid Urbanization in the Shenzhen River Catchment: An Integrated View of Socio-Economic and Infrastructure Development. *Sustainability* **2014**, *6*, 7433−7451.

(4) Martínez-Huitle, C. A.; Brillas, E. Decontamination of wastewaters containing synthetic organic dyes by electrochemical methods: A general review. *Appl. Catal., B* **2009**, *87*, 105−145.

(5) Ribeiro, A. R.; et al. An overview on the advanced oxidation processes applied for the treatment of water pollutants defined in the recently launched Directive 2013/39/EU. *Environ. Int.* **2015**, *75*, 33−51.

(6) Khan, M. Z.; et al. Microbial electrolysis cells for hydrogen production and urban wastewater treatment: A case study of Saudi Arabia. *Appl. Energy* **2017**, *185*, 410−420.

(7) Tesh, S. J.; Scott, T. B. Nano-composites for water remediation: a review. *Adv. Mater.* **2014**, *26*, 6056−6068.

(8) Särkkä, H.; Bhatnagar, A.; Sillanpää, M. Recent developments of electro-oxidation in water treatment — A review. *J. Electroanal. Chem.* **2015**, *754*, 46−56.

(9) Andreozzi, R. Advanced oxidation processes (AOP) for water purification and recovery. *Catal. Today* **1999**, *53*, 51−59.

(10) Eduardo da Hora Machado, A.; et al. Solar photo-Fenton treatment of chip board production waste water. *Sol. Energy* **2004**, *77*, 583−589.

(11) Pasternak, S.; Paz, Y. On the similarity and dissimilarity between photocatalytic water splitting and photocatalytic degradation of pollutants. *ChemPhysChem* **2013**, *14*, 2059−2070.

(12) Kötz, R.; Stucki, S.; Carcer, B. Electrochemical waste water treatment using high overvoltage anodes. Part I: Physical and electrochemical properties of SnO2 anodes. *J. Appl. Electrochem.* **1991**, *21*, 14−20.

(13) Higgins, M. W.; et al. Carbon fabric based solar steam generation for waste water treatment. *Sol. Energy* **2018**, *159*, 800−810.

(14) Perez-Rodriguez, P.; et al. Treatment of Organic Pollutants Using a Sol. Energy Driven Photo-Oxidation Device. *Adv. Sustainable Syst.* **2017**, *1*, No. 1700010.

(15) Zhang, L.-W.; et al. Synthesis of Porous Bi2WO6Thin Films as Efficient Visible-Light-Active Photocatalysts. *Adv. Mater.* **2009**, *21*, 1286−1290.

(16) Sun, S.; Wang, W. Advanced chemical compositions and nanoarchitectures of bismuth based complex oxides for solar photocatalytic application. *RSC Adv.* **2014**, *4*, 47136−47152.

(17) Al-Hamdi, A. M.; et al. Efficient photocatalytic degradation of phenol in aqueous solution by SnO 2:Sb nanoparticles. *Appl. Surf. Sci.* **2016**, *370*, 229−236.

(18) Smith, W.; Zhao, Y. P. Superior photocatalytic performance by vertically aligned core−shell TiO2/WO3 nanorod arrays. *Catal. Commun.* **2009**, *10*, 1117−1121.

DOI: 10.1021/acsomega.8b02502
ACS Omega 2018, 3, 14392−14398

(19) Zeng, Q.; et al. Highly-stable and efficient photocatalytic fuel cell based on an epitaxial TiO2/WO3/W nanothorn photoanode and enhanced radical reactions for simultaneous electricity production and wastewater treatment. *Appl. Energy* **2018**, *220*, 127−137.
(20) Ghaly, M. Y.; et al. Treatment of highly polluted paper mill wastewater by solar photocatalytic oxidation with synthesized nano TiO2. *Chem. Eng. J.* **2011**, *168*, 446−454.
(21) Sreeja, S.; Shetty, K. V. Photocatalytic water disinfection under solar irradiation by Ag@TiO 2 core-shell structured nanoparticles. *Sol. Energy* **2017**, *157*, 236−243.
(22) Perez-Rodriguez, P.; et al. Treatment of Organic Pollutants Using a Sol. Energy Driven Photo-Oxidation Device. *Adv. Sustainable Syst.* **2017**, *1*, No. 1700010.
(23) Shen, Z.; et al. Degradation of dye solution by an activated carbon fiber electrode electrolysis system. *J. Hazard. Mater.* **2001**, *84*, 107−116.
(24) Tyagi, V. V.; et al. Progress in solar PV technology: Research and achievement. *Renewable Sustainable Energy Rev.* **2013**, *20*, 443−461.
(25) Huang, J.; Shao, Y.; Dong, Q. Organometal Trihalide Perovskite Single Crystals: A Next Wave of Materials for 25% Efficiency Photovoltaics and Applications Beyond? *J. Phys. Chem. Lett.* **2015**, *6*, 3218−3227.
(26) Yang, J.; Banerjee, A.; Guha, S. Amorphous silicon based photovoltaics—from earth to the "final frontier". *Sol. Energy Mater. Sol. Cells* **2003**, *78*, 597−612.
(27) Cotal, H.; et al. III−V multijunction solar cells for concentrating photovoltaics. *Energy Environ. Sci.* **2009**, *2*, 174−192.
(28) Siddiki, M. K.; et al. A review of polymer multijunction solar cells. *Energy Environ. Sci.* **2010**, *3*, 867.
(29) Zareie, M. H.; Körbahti, B. K.; Tanyolaç, A. Non-passivating polymeric structures in electrochemical conversion of phenol in the presence of NaCl. *J. Hazard. Mater.* **2001**, *87*, 199−212.
(30) Lizhang, W.; et al. The influence of anode materials on the kinetics toward electrochemical oxidation of phenol. *Electrochim. Acta* **2016**, *206*, 270−277.
(31) Bennani, Y.; Appel, P.; Rietveld, L. C. Optimisation of parameters in a solar light-induced photoelectrocatalytic process with a TiO2/Ti composite electrode prepared by paint-thermal decomposition. *J. Photochem. Photobiol., A* **2015**, *305*, 83−92.
(32) Singhal, G. S.; Rabinowitch, E. Changes in the absorption spectrum of methylene blue with pH. *J. Phys. Chem.* **1967**, *71*, 3347−3349.
(33) An, T. C.; Zhu, X. H.; Xiong, Y. Feasibility study of photoelectrochemical degradation of methylene blue with three-dimensional electrode-photocatalytic reactor. *Chemosphere* **2002**, *46*, 897−903.
(34) Umebayashi, T.; et al. Visible Light-Induced Degradation of Methylene Blue on S-doped TiO2. *Chem. Lett.* **2003**, *32*, 330−331.
(35) Staebler, D. L.; Wronski, C. R. Reversible conductivity changes in discharge-produced amorphous Si. *Appl. Phys. Lett.* **1977**, *31*, 292−294.
(36) Daskalaki, V. M.; et al. Solar light-induced photoelectrocatalytic degradation of bisphenol-A on TiO2/ITO film anode and BDD cathode. *Catal. Today* **2013**, *209*, 74−78.
(37) Li, X. Y.; et al. Reaction pathways and mechanisms of the electrochemical degradation of phenol on different electrodes. *Water Res.* **2005**, *39*, 1972−81.
(38) Wang, Q.; Tian, S.; Ning, P. Degradation Mechanism of Methylene Blue in a Heterogeneous Fenton-like Reaction Catalyzed by Ferrocene. *Ind. Eng. Chem. Res.* **2014**, *53*, 643−649.
(39) Yang, G.; et al. A novel way of texturing glass for microcrystalline silicon thin film solar cells application. *Prog. Photovoltaics: Res. Appl.* **2015**, *23*, 1283−1290.
(40) Autolab, M. Autolab PGSTAT302N-High Performance, 2018. Available at https://www.metrohm.com/en/products/electrochemistry/autolab-modular-line/PGSTAT302N.
(41) Company, H. *DR5000 Spectrophotometer - Procedures Manual*, 2005.
(42) Panizza, M.; et al. Electrochemical degradation of methylene blue. *Sep. Purif. Technol.* **2007**, *54*, 382−387.

DOI: 10.1021/acsomega.8b02502
ACS Omega 2018, 3, 14392−14398